Fermi National Accelerator Laboratory

FERMILAB-Pub-93/083-E

E705

Production of Chi Charmonium via 300 GeV/c Pion and Proton Interactions on a Lithium Target

L. Antoniazzi et al
the E705 Collaboration

Fermi National Accelerator Laboratory
P.O. Box 500, Batavia, Illinois 60510

April 1993

Submitted to *Physical Review Letters*

Disclaimer

Production of Chi Charmonium via 300 GeV/c Pion and Proton Interactions on a Lithium Target

L. Antoniazzi[3], M. Arenton[9], Z. Cao[8], T. Chen[5], S. Conetti[4], B. Cox[9], S. Delchamps[3], L. Fortney[2], K. Guffey[7], M. Haire[4], P. Ioannou[1], C. M. Jenkins[3], D. J. Judd[7], C. Kourkoumelis[1], A. Manousakis-Katsikakis[1], J. Kuzminski[4], T. LeCompte[6], A. Marchionni[4], M. He[8], P. O. Mazur[3], C. T. Murphy[3], P. Pramantiotis[1], R. Rameika[3], L. K. Resvanis[1], M. Rosati[4], J. Rosen[6], C. Shen[8], Q. Shen[2], A. Simard[4], R. P. Smith[3], L. Spiegel[3], D. G. Stairs[4], Y. Tan[6], R. J. Tesarek[2], T. Turkington[2], L. Turnbull[7], F. Turkot[3], S. Tzamarias[6], G. Voulgaris[1], D. E. Wagoner[7], C. Wang[8], W. Yang[3], N. Yao[5], N. Zhang[8], X. Zhang[8], G. Zioulas[4], B. Zou[2]

(E705 Collaboration)

(1) University of Athens, Athens, Greece
(2) Duke University, Durham, NC 27708-0305
(3) Fermi National Accelerator Laboratory, Batavia, IL 60510
(4) McGill University, Montreal, PQ, Canada H3A 2T8
(5) Nanjing University, Nanjing, People's Republic of China
(6) Northwestern University, Evanston, IL 60208
(7) Prairie View A&M University, Prairie View, TX 77445
(8) Shandong University, Jinan, Shandong, People's Republic of China
(9) University of Virginia, Charlottesville, VA 22901

Abstract

We present a measurement and comparison of the χ_{c1} and χ_{c2} production cross sections determined from interactions of 300 GeV/c $\pi^{\pm}$ and p with a Li target. We find χ_{c1}/χ_{c2} production ratios of $0.52^{+0.57}_{-0.27}$ and $0.08^{+0.25}_{-0.15}$ from reactions induced by $\pi^{\pm}$ and p respectively.

PACS numbers 13.85.Qk, 14.40.Gx

The production of χ_c states has been widely described as proceeding through the interaction of valence quarks or gluons[1-5] in the context of two models, color singlet and color evaporation, that make significantly different predictions for the

production ratios of the three χ_c states. In particular, the color singlet, gluon fusion model predicts little or no production of the χ_{c1} state, while the color singlet and evaporation models for light quark annihilation predict χ_{c1}/χ_{c2} production ratios of 4:1 and 3:5 respectively[3]. There have been several tests of these predictions in π^- beams[6-9] but only one previous study using a proton beam[9].

The χ_c mesons studied here are observed in the decay mode $J/\psi + \gamma$ and were produced in Fermilab experiment E705 in the interactions of 300 GeV/c tagged positive and negative beams incident on a 33 cm long lithium target. The open geometry, single analyzing magnet spectrometer included both MWPCs and drift chambers and was followed by an electromagnetic shower detector[10, 11] and a muon detector. We triggered on a di-muon mass greater than 2.4 GeV/c^2 and obtained approximately 25,000 J/ψ events[12] above background.

The shower detector covered an area of 3.7×2.0 m^2 10 m downstream of the target. It consisted of an "active converter" plane fronting a "main array" of 228 lead (SF5) and 164 scintillating (SCG1-C) glass blocks. The active converter plane was composed of a lead/gas tube sampling device (LGC) covering the central 1.03 m section and arrays of vertical SCG1-C blocks followed by a gas tube hodoscope (GTH) in the outer regions. The LGC and the GTH were able to measure both x and y shower positions.

The energy determination for photons from the $\chi_c \rightarrow J/\psi + \gamma$ decay is critical to the identification of the decay as being from χ_{c1} or χ_{c2}. The shower detector was calibrated at approximately monthly intervals during the run by exposing each block in the calorimeter to electron beams at nominal energies of 6, 10, 30, 60, and 100 GeV. An LED light pulsing system[11] provided gain tracking between calibrations and between the analysis magnet-off calibration condition and the magnet-on data acquisition condition. To determine energy dependent gains for the SCG1-C blocks and their photomultiplier tubes that were not dependent on the nominal beam momentum settings, we made the assumption that the gains of the SF5 elements had no energy dependence. For all main array blocks, we also determined energy-dependent shower depth correction factors based on the energy deposit in the active converter.

The overall energy scale was set by subsequent studies of the distribution of the ratio of energy/momentum (E/p) of approximately 160,000 $e^{\pm}$ tracked by the spectrometer. With this procedure we determined the calibration beam energies to be 6.6, 10.7, 31.5, 61.0, and 101.2 GeV.

In all non-calibration triggers, a significant intensity dependent energy offset was observed in the digitized data from the main array glass elements of the calorimeter. This offset was proportional to the average power deposited in a block, and we were able to remove most of it using other recorded information associated with each event. The remnants of this offset were ultimately removed using the E/p studies, but fluctuations about its mean value significantly degraded the resolution of the calorimeter.

In addition to cuts imposed by the tracking program[12, 13], the J/ψ sample was selected by requiring that $2.98 < M(\mu^+\mu^-) < 3.18$ GeV and a vertex z inside the target. Electromagnetic shower candidates were required to develop in live regions of the detector, to have a hit in the position hodoscopes with an active converter energy greater the 200 MeV, and to have a total energy greater than 1 GeV. Showers that were used to form $M(\mu\mu\gamma)$ were further required to have a good fit to an electromagnetic shower profile, no charged track within 6 cm, an active converter energy greater than 400 MeV, a total energy greater than 2.5 GeV, and no combination with another electromagnetic shower candidate forming a $M(\gamma\gamma)$ less than 200 MeV/c^2. Figure 1 a,b shows the $M(\mu^+\mu^-\gamma)$ - $M(\mu^+\mu^-)$ mass distributions[14] for $\pi^\pm$ and p beams.

We generate a background b_i for each mass difference plot by mispairing each accepted γ with the J/ψ from each of the other events that appear on the plot, removing unwanted contributions that arise when the γ comes from a χ_c decay[15]. The background shapes also include contributions from ψ' --> J/ψ π^0 π^0 and ψ' --> J/ψ η decays. The background shapes are then fit to a ninth-order polynomial and normalized to one.

Using the likelihood method, we perform a simultaneous fit to two mass plots ($\pi^\pm$ and p beam) identified by the subscript i in the probability function of the kth event

$$l_k = \frac{R_i N_i}{R_i + 1} p_1(M) + \frac{N_i}{R_i + 1} p_2(M + 45.7 \text{ MeV}) + B_i b_i \ ,$$

where p_1 and p_2 are the resolution functions of the χ_{c1} and χ_{c2} resonances, and the b_i describe the unity normalized background distributions on each of the plots. There are seven free parameters: M is the mass of the χ_{c1} resonance, and in each of the beam-type samples, N_i is the total number of observed $\chi_{c1} + \chi_{c2}$ decays to $\mu^+\mu^-$, R_i is the ratio χ_{c1}/χ_{c2} of these decays, and B_i is the number of background events.

With n as the total number of events, we modify the extended likelihood function[16]

$$L = \frac{e^{-\Sigma(N_i+B_i)}}{n!} g\left(\frac{M-M_1}{\sigma}\right)\prod_{k=1}^{n} l_k$$

to include a Gaussian factor g describing the uncertainty of our mass scale. In this function M_1 = 3510.5 and σ =6.0 MeV/c^2 corresponding to the 1.5% uncertainty in the photon energy scale indicated by our electron and π^0 studies.

The χ_c resolution functions, p_1 and p_2, are derived from a Monte Carlo sample of χ_c events that were generated to have the x_F and p_T distributions of our measured J/ψ events then weighted by acceptances and efficiencies. Measurement errors were folded into these events at the hit level for charged tracks and at the energy and position level for photon showers. The solid curves in Figure 2 show the corresponding resolution functions for $e^{\pm}$ energy and π^0 mass determined using the same error assignment methods used for the χ_c.

The results from this simultaneous likelihood fit to the plots in Figure 1 are given in the first two lines of Table I. The fitted mass M of the χ_{c1} is 3511.5 ± 5.6 MeV/c^2. Because the χ_c states are not cleanly separated, the ratios R_i are strongly correlated with the fitted mass M: these ratios are otherwise insensitive to systematic effects.

Table I. The parameters for the fits on Figure 1 for the total number of χ_c mesons and the ratio χ_{c1}/χ_{c2} seen decaying to J/ψ. The errors are statistical only.

	N	R
p	244 ± 56	$0.17^{+0.51}_{-0.31}$
$\pi\pm$	632 ± 84	$1.06^{+1.16}_{-0.55}$

When the known branching ratios to J/ψ + γ are applied (27.3 ± 1.6% and 13.5 ± 1.1% for χ_{c1} and χ_{c2} respectively[17]), we find the ratio of produced χ_1/χ_2 to be $0.52^{+0.57}_{-0.27}$ for the $\pi^{\pm}$ beam and $0.08^{+0.25}_{-0.15}$ for the p beam. From a similar likelihood fit parameterized in terms of the number of χ_{c1} and χ_{c2} decays seen, we obtain the highly anticorrelated estimates for the inclusive cross sections shown in Table II.

Table II. The inclusive cross sections for $\pi^{\pm}$ and p induced reactions.

	$\sigma\chi_1$ (nb)	$\sigma\chi_2$ (nb)	Correlation
$\pi\pm$	$146 \pm 55 \pm 15$	$277 \pm 115 \pm 28$	-0.74
p	$31 \pm 62 \pm 3$	$364 \pm 124 \pm 36$	-0.66

Figure 3 shows the acceptance and efficiency corrected, and background subtracted, invariant differential cross sections for inclusively produced χ_c's from $\pi^{\pm}$ and p induced reactions. The vertical scale is set using the χ_{c1}/χ_{c2} production ratios reported here, but the errors shown on the figures are statistical only and do not include the uncertainty in this ratio. The curves on these plots are fits to the functions $d\sigma/d\,p_T^2 = Ae^{ap_T}$ and $d\sigma/dx_F = A\left(1-\left(x_F - x_0\right)^2\right)^b$. Table III displays the parameters of these fits and one to $d\sigma/dx_F = A\left(1-|x-x_c|\right)^c$. This table also displays α from a fit of the expression[2] $dN/d\cos\vartheta = \left(1+\alpha\cos^2\vartheta\right)$ to the photons in the χ_c signal, where ϑ is the angle between the μ^+ and beam momenta in the in the χ_c rest frame. The distributions in $\cos\vartheta$ are consistent with isotropy.

Table III. The fitted coefficients describing the invariant cross sections and decay photon distribution for $\pi^{\pm}$ and p induced reactions.

	$\pi\pm$	p
a (c/GeV)	$-1.39 \pm .14$	$-1.47 \pm .25$
x_0	0.19 ± 0.07	0.13 ± 0.05
b	7.7 ± 6.4	18 ± 14
x_c	0.22 ± 0.14	0.13 ± 0.09
c	2.0 ± 2.7	4.6 ± 4.7
α	0.9 ± 1.5	1.8 ± 2.1

Our χ_{c1}/χ_{c2} production ratio for pion production is in agreement with an earlier determination[7] (compare 0.72 ± 0.25 with R in Table I), but since both quark and gluon processes are possible these results do not select a specific model. The ratio for proton production is less well known[9], and our result favors the color-singlet two-gluon model for χ_c production. However this color-singlet model does

not permit significant J/ψ production, and we note that a previously published study[12] of this data found that 60% of the J/ψ seen in proton interactions are likely to be directly produced.

This work was supported in part by the U.S. Department of Energy, the Natural Sciences and Engineering Research Council of Canada, the Quebec Department of Education, and the Scientific Affairs Division of the North Atlantic Treaty Organization. We also wish to thank the administration and staff of the Fermi National Accelerator Laboratory.

References

1 R. Barbieri and R. Gatto, Phys. Lett. **61B**, 465 (1976).

2 B. L. Ioffe, Phys. Rev. Lett. **39**, 1589 (1977).

3 J. H. Kühn, Phys. Lett. **89B**, 385 (1980).

4 R. Barbieri, *et al.*, Phys. Lett. **60B**, 183 (1976).

5 C. E. Carlson and R. Suaya, Phys. Rev. D **15**, 1416 (1977).

6 T. B. Kirk, *et al.*, Phys. Rev. Lett. **42**, 619 (1979).

7 Y. Lemoigne, *et al.*, Phys. Lett. **113B**, 509 (1982).

8 S. R. Hahn, *et al.*, Phys. Rev. D **30**, 671 (1984).

9 D. A. Bauer, *et al.*, Phys. Rev. Lett. **54**, 753 (1985).

10 L. Antoniazzi, *et al.*, Submitted to Nucl. Instr. Methods A. (1993).

11 T. Turkington, Ph.D. thesis, Duke University, 1989; M. Rosati, Ph. D. thesis, McGill University, 1992; R. Tesarek, Ph. D. thesis, Duke University, 1993.

12 L. Antoniazzi, *et al.*, Phys. Rev. Lett. **70**, 383 (1993).

13 L. Antoniazzi, *et al.*, Phys. Rev. D **46**, 4829 (1993).

14 These mass distributions are different in detail from those of our previous paper as a result of tighter cuts and a reanalysis of the energy corrections. These differences do not affect the conclusions of the earlier paper. The $M(\mu^+\mu^-)$ distributions are unchanged.

15 These events produce a distribution with an enhancement near the χ mass which we generate by a second mispairing after weighting each photon by the probability that it came from a χ decay.

16 F. T. Solmitz, Ann. Rev. Nucl. Sci. **14**, 375 (1964).

17 D. M. Aguilar-Benitez Doe, Physical Review **45D**, (1992).

Figure Captions

Figure 1. Distributions of $M(\mu^+\mu^-\gamma)$ - $M(\mu^+\mu^-)$ for $\pi^\pm$ and p induced reactions. The smooth curves are from the likelihood fit, and the insets show the background subtracted χ_c signal.

Figure 2. Distribution of (a) E/p for tracks pointing to electromagnetic showers and (b) $M(\gamma\gamma)$ for all events with an identified J/ψ. Clear signals are seen for produced $e^\pm$ and π^0 particles. The curves show the expected distributions based on our measurement errors.

Figure 3. Differential cross sections for χ_c from $\pi^\pm$ and p induced reactions.

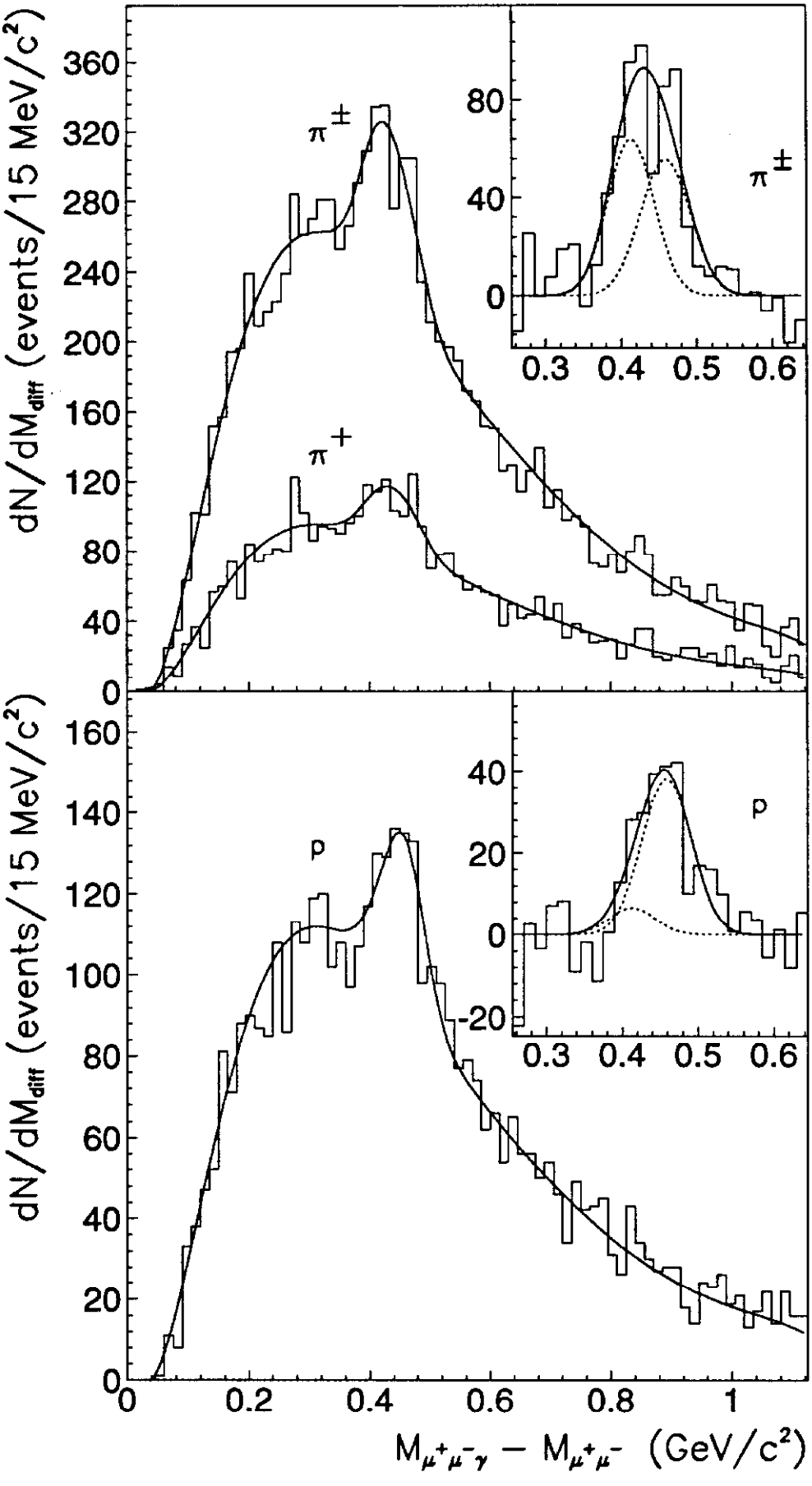

Fig. 1

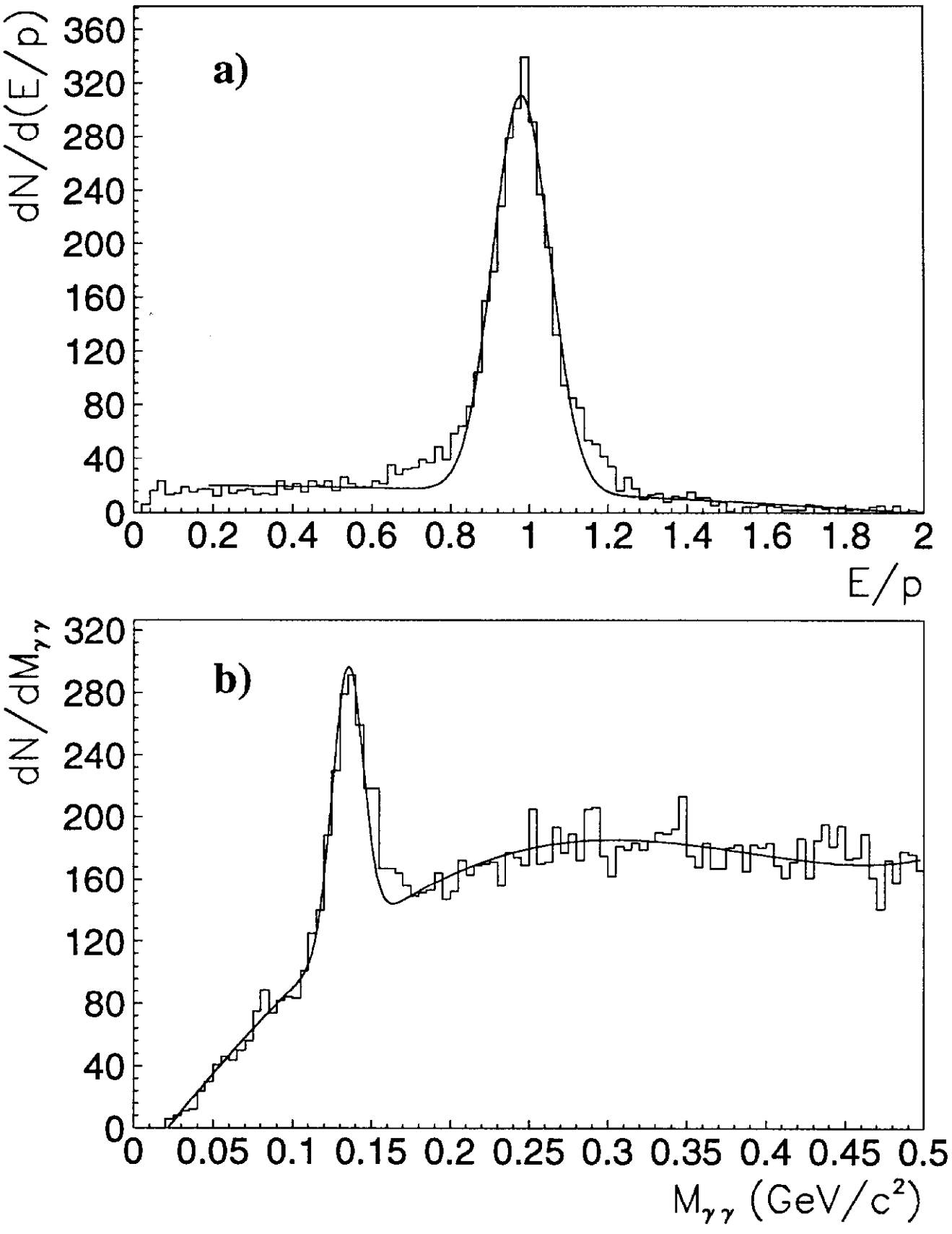
a)
dN/d(E/p)
360
320
280
240
200
160
120
80
40
0
0
0.2
0.4
0.6
0.8
1
1.2
1.4
1.6
1.8
2
E/p
b)
dN/dM$_{\gamma\gamma}$
320
280
240
200
160
120
80
40
0
0
0.05
0.1
0.15
0.2
0.25
0.3
0.35
0.4
0.45
0.5
M$_{\gamma\gamma}$ (GeV/c^2)

Fig. 2

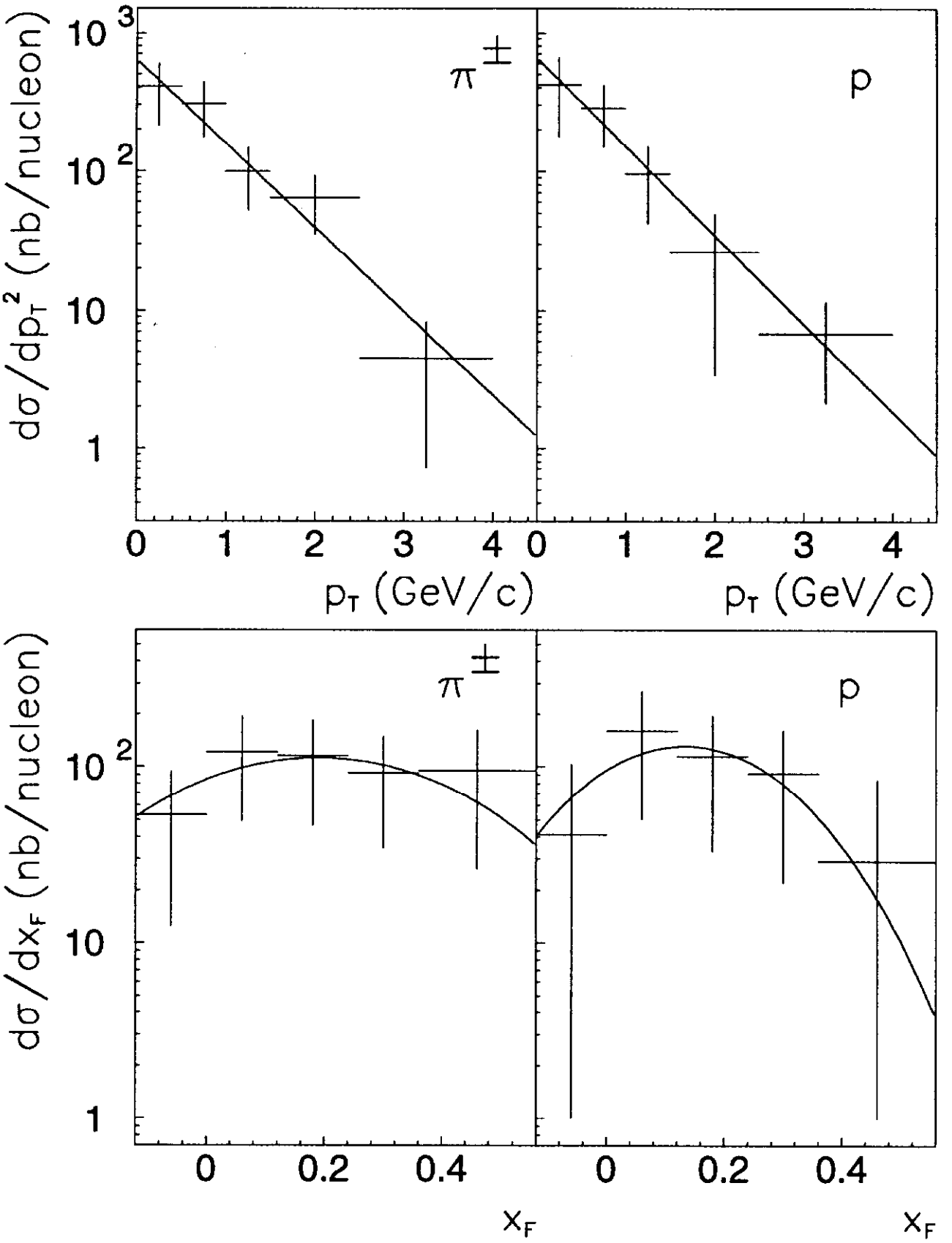
$d\sigma/dp_T^2$ (nb/nucleon)
10^3
10^2
10
1
$\pi^{\pm}$
p
0 1 2 3 4
p_T (GeV/c)
$d\sigma/dx_F$ (nb/nucleon)
10^2
10
1
0 0.2 0.4
x_F

Fig. 3